Journal of Computer-Aided Molecular Design (2006) 19: 871–885
DOI 10.1007/s10822-005-9030-2

Protein farnesyltransferase: Flexible docking studies on inhibitors using computational modeling

Wayne C. Guida[a,b,*], Andrew D. Hamilton[c], Justin W. Crotty[b] & Saïd M. Sebti[a]
[a]*Drug Discovery Program, H. Lee Moffitt Cancer Center & Research Institute, Departments of Oncology and Biochemistry & Molecular Biology, College of Medicine, University of South Florida, Tampa, FL, 33612, USA;* [b]*Department of Chemistry, Eckerd College, St. Petersburg, FL, 33711, USA;* [c]*Department of Chemistry, Yale University, 208107 New Haven, CT, 06520, USA*

Received 5 May 2005; accepted 9 November 2005

Key words: docking, drug design, flexible docking, molecular modeling, protein farnesyltransferase

Summary

Using MacroModel, peptide, peptidomimetic and non-peptidomimetic inhibitors of the zinc metalloenzyme, farnesyltransferase (FTase), were docked into the enzyme binding site. Inhibitor flexibility, farnesyl pyrophosphate substrate flexibility, and partial protein flexibility were taken into account in these docking studies. In addition to CVFM and CVIM, as well as our own inhibitors FTI-276 and FTI-2148, we have docked other farnesyltransferase inhibitors (FTIs) including Zarnestra, which presently is in advanced clinical trials. The AMBER* force field was employed, augmented with parameters that were derived for zinc. A single binding site model that was derived from the crystal structure of CVFM complexed with farnesyltransferase and farnesylpyrophosphate was used for these studies. The docking results using the lowest energy structure from the simulation, or one of the lowest energy structures, were generally in excellent agreement with the X-ray structures. One of the most important findings of this study is that numerous alternative conformations for the methionine side chain can be accommodated by the enzyme suggesting that the methionine pocket can tolerate groups larger than methionine at the C-terminus of the tetrapeptide and suggesting alternative locations for the placement of side chains that may improve potency.

Introduction

The enzyme, protein farnesyltransferase (FTase), has received considerable attention over the past several years due to the potential role of inhibitors of this enzyme (FTIs) as anti-cancer agents [1–4]. FTase catalyzes the first step in post-translational modifications of the *Ras* oncoprotein, and other proteins that are believed to play a pivotal role in carcinogenesis. FTase catalyzes the transfer of the 15-carbon isoprene-based farnesyl group from farnesylpyrophosphate (FPP) to the sulfur atom of a cysteine residue in the CaaX sequence located at the C-terminus of *Ras* and other proteins (where *a* refers to an aliphatic amino acid and *X* refers to an uncharged amino acid). In subsequent post-translational steps, the aaX peptide is removed via proteolysis and the resulting farnesylated C-terminal cysteine carboxyl group is methylated to the methyl ester. The farnesyl group, now attached to the C-terminal cysteine via a thioether linkage

*To whom correspondence should be addressed. E-mail: guidawc@moffitt.usf.edu

serves to anchor the *Ras* protein to the inner surface of the plasma membrane, which is essential for the function of *Ras*. Oncogenic mutations in the *ras* gene occur in approximately 30% of all human cancers, which results in aberrant cellular signaling, and inhibitors of FTase could potentially ameliorate this abnormality. In fact, it has been demonstrated that FTIs inhibit human tumor growth and some efficacy has also been observed in clinic trials [2]. It is worth noting, however, that the observed biological effects of FTIs appear to be far more complicated than simple inhibition of *Ras* farnesylation [3].

A number of X-ray structures have been reported for FTase, including the structures of complexes with several different inhibitors [5–14]. The mammalian enzyme exists as a heterodimer and the α-subunit of the rat enzyme, which has been extensively studied crystallographically, contains 377 residues, whereas the β-subunit contains 437 residues. FTase is a zinc metalloenzyme with a Zn^{2+} ion ligated to a histidine, cysteine and aspartate (His362β, Cys299β and Asp297β).

We have had a long-standing interest in preparing FTIs as potential anti-cancer agents and have utilized crystallographic information in the design of some of these inhibitors [15]. We wished to further our understanding of the SAR of inhibitors prepared in our laboratories (and those of others) in order to design new inhibitors that are more efficacious. Thus, we conducted molecular modeling studies involving docking of a number of FTIs to FTase. We have docked inhibitors for which crystallographic information is available in order to test and validate the methodology that would be effective for a zinc metalloenzyme such as FTase. We also docked inhibitors for which such crystallographic information was unavailable upon initiation of our study to determine the likely binding mode of these compounds. Herein we report the results of our studies.

Computational methods

All of the docking studies were performed using the MacroModel 7.0 software [16]. Both the Maestro GUI and the original MacroModel GUI were used as an interface to MacroModel (previously referred to as BatchMin). The ''Low Mode'' docking search method [17] available within MacroModel was employed for our flexible docking studies and *inhibitor flexibility, FPP substrate flexibility and partial protein flexibility* were taken into account. All of the calculations were performed on an SGI R5000 O2 workstation running Irix 6.5 and/or an Intel Linux cluster incorporating four Pentium III 650 MHz CPUs running RedHat Linux 7.0. Some of the jobs were distributed over multiple processors on the Linux cluster. The FLO96 software [18] was used for visualizing ''extra radius'' accessible surfaces [19]. Graphics images were rendered using either Viewer Lite 5.0 [20] or Maestro.

Force field

The AMBER* force field was employed for all of the flexible docking simulations reported. Neither an explicit nor implicit solvation model was employed for our simulations but dielectric screening was handled by using a distance dependent dielectric model for the electrostatic potential energy calculations. Both 2r and 4r distance dependent electrostatics were tested. Parameters for zinc were initially taken from our prior work on thermolysin [21]. Note that in our model, like the one described by Hoops, Anderson and Merz [22], all of the torsional parameters associated with the zinc ligand bonds were set to zero. We decided to utilize a model for zinc in which its protein ligands are directly bonded to zinc [22], but we have used a non-bonded model for ligation to zinc for all of the inhibitors studied. In this non-bonded model, only electrostatic and van der Waals forces govern ligation of the inhibitors to zinc. The Jaguar program [23] was employed to calculate charges for zinc and its neighboring ligands by fitting the partial charges to the electrostatic potential calculated at the B3LYP density functional level with the LACVP* basis set. For this calculation, a truncated model for the catalytic site of FTase (taken from the Protein Databank [24], entry: 1JCR) was employed that utilized all residues that were within a 4 Å shell surrounding the zinc ion in the catalytic site. Thus, residues Asp297β, Cys299β, Tyr361β and His362β were included in the calculation along with the cysteine of the tetrapeptide inhibitor CVFM that was present in the co-crystallized structure. Gly298β was also included in the calculation (in addition to Asp297β and Cys299β) to form a complete

tripeptide fragment. The residues were extended out in each direction to the α-carbon atom of the adjacent residue and hydrogen atoms were added using the original MacroModel GUI. The N-terminal amino group of the cysteine from CVFM was protonated and the cysteine thiols were unprotonated. After obtaining the charges, the stretching and bending parameters for the zinc-heteroatom bonds and van der Waals parameters for zinc were tweaked manually (but only slightly relative to the initial parameters) to improve the geometry of CVFM docked into its "own" binding site using the simulation methodology described below.

Protein preparation

The enzyme structure used for the docking studies was derived from the X-ray structure [10] of rat FTase determined at 2.0 Å resolution with the peptide CVFM and FPP bound to the catalytic site (1JCR from the Protein Databank [24]). Polar hydrogens, aromatic hydrogens on Phe, Trp and Tyr resides within 10 Å of zinc, and sulfur lone pairs were added to the structure. The protein structure was refined for the docking calculations by subjecting it to successive rounds of energy minimization using a parabolic restraining potential. The initial force constant for the restraining potential was 500 kJ/Å^2. The steepest descent minimizer was used for energy minimization. During successive rounds of energy minimization, the force constant was gradually reduced by a factor of *ca.* 2 until it had reached a value of 5 kJ/Å^2 for the final round of energy minimization. Cys299β and inhibitor cysteines were modeled as thiolates.

Simulation details

Each flexible docking simulation consisted of 10,000 steps of the Low Mode docking search procedure [17], in which both positional/orientational sampling as well as conformational sampling can be performed. In addition to the peptide inhibitors CVFM and CVIM, the inhibitors shown in Figure 1 were studied. Amino groups of the inhibitors were protonated and carboxylic acids were deprotonated. *All of the inhibitors were docked into the 1JCR binding site model.* The protein was truncated to a 20 Å shell of complete residues surrounding the zinc ion and extended out to the α-carbon of the adjacent residue in both directions. Residues (side chain and backbone atoms) within 4 Å of zinc (as described above for force field parameterization), zinc itself, FPP, and each inhibitor were fully flexible during the docking procedure, which consisted of structural perturbation followed by energy minimization. All other residues were frozen at their positions after

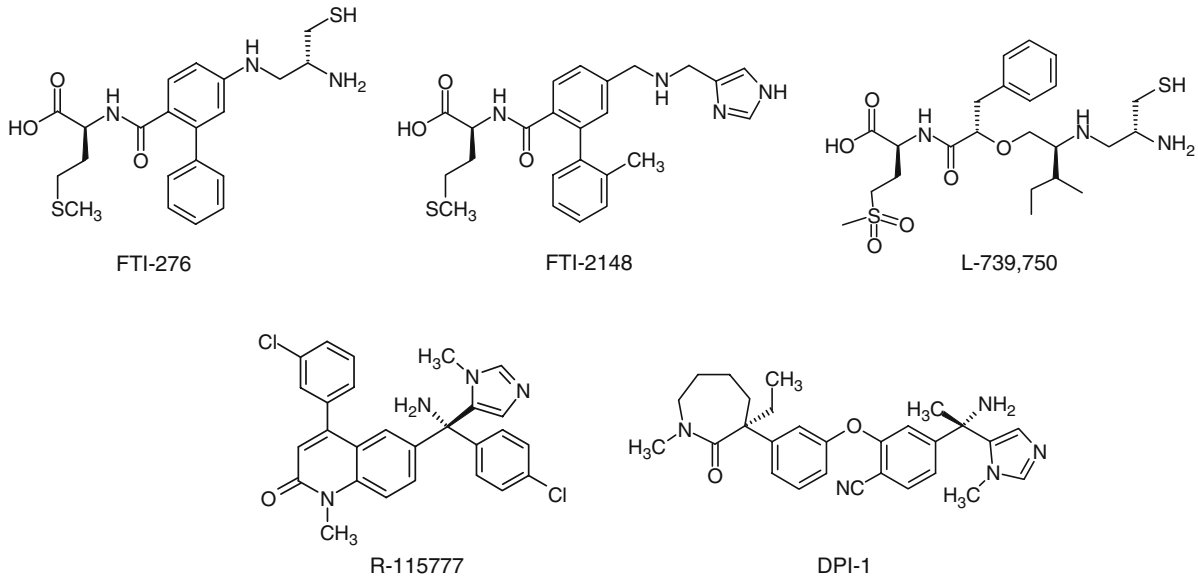

Figure 1. Compounds used for this study in addition to CVFM and CVIM.

refinement (see *Protein Preparation*, above). Thus, only the van der Waals and electrostatic potentials of these residues interacting with the flexible residues contributed to the overall potential energy (with suitable handling of boundary residues by the MacroModel program).

Conformational sampling with the Low Mode procedure operates by following trajectories taken from the low frequency modes of vibration of the FTase/FPP/inhibitor ternary complexes. Positional/orientational moves and explicit torsional rotations for freely rotatable bonds were used for each inhibitor to augment the conformational sampling performed by the Low Mode procedure. The energy minimization phase of the docking procedure was accomplished by using the truncated Newton conjugate gradient minimizer. The inhibitors studied were generally positioned in an arbitrary pose (i.e., position, orientation and conformation)[1] within the catalytic site and the usage directed procedure [25] was then used to select the starting structure for each subsequent Low Mode docking step. The lowest energy structure (LES) and all unique[2] low energy structures within 25 kJ/mol of the lowest energy structure were saved for further analysis. Entropic factors were not considered in our docking simulations.

Results and discussion

Peptide inhibitors

CVFM

In the first docking study, CVFM was docked into its "own" binding site. CVFM was adjusted manually into an arbitrary pose[1] within the FTase binding site using Maestro to initiate the docking run. FPP started at its crystallographic position but was free to move during the energy minimization phase of the docking maneuver. Initial docking studies were conducted using both 2r and 4r electrostatics. Although the initial simulations with 2r electrostatics produced structures that were in substantial agreement with the X-ray structure, docking simulations were subsequently performed with a starting structure that involved an extended backbone conformation of CVFM (as observed crystallographically) that had been rotated within the catalytic site so that the methionine residue was close to the zinc ion and the cysteine residue was within the Met binding pocket. Such a starting structure places the cysteine thiol in a location that is quite remote from the zinc ion to which it ultimately binds. This starting structure also possessed side chain conformations that were rotated relative to the X-ray structure and the docking simulation produced an ensemble of low energy structures (within a 25 kJ energy window) that did not contain any structures resembling the X-ray structure. The structures produced were all lower energy than the lowest energy structure (LES) from our previous searches and lower energy than the pose obtained by subjecting the structure observed crystallographically to energy minimization. On the other hand, several simulations using 4r electrostatics initiated with different starting structures did produce ensembles of structures that contained docked poses that closely resembled the X-ray structure.[3] For example, a simulation employing 4r electrostatics, but otherwise identical to the one described above that employed 2r electrostatics with CVFM "flipped" within the catalytic site, produced an ensemble of structures that contained structures resembling the crystal structure.[4] In this simulation, the LES showed reasonable agreement with the X-ray structure. In Table 1 we show our results for CVFM (and other inhibitors). These results include the RMSDs for overlaying the X-ray structure of the inhibitor on the LES (and, if not the LES, on the structure within 10 kJ/mol that exhibited the best fit to the X-ray structure) and calculating the RMSD of corresponding non-hydrogen atoms, herein referred to as overlay RMSDs. CVFM in the LES binds in an extended conformation with the cysteine thiol ligated to zinc as is observed crystallographically and possesses an overlay RMSD of 1.40 Å when compared to the X-ray structure. In Table 1 we also show the RMSD (1.23 Å, for the CVFM LES) that was obtained when the docked inhibitor was rigidly aligned (using non-hydrogen atoms) on the X-ray structure of the inhibitor that was used as a template, using least-squares superimposition, herein referred to as a superimposition RMSD. This number indicates how well the *conformation* of the docked inhibitor matches the one observed crystallographically and reflects the contribution of the docked conformation to the overall pose. Figure 2a shows the resulting LES. CVFM and several key residues in the FTase binding site, as

Table 1. RMS deviations of the docked vs. the crystallographically determined structures of inhibitors used in this study.

Inhibitor	Rank	RMSD (Å)[a]	Relative energy (kJ)	Total number of poses[b]
CVFM	1	1.40 (1.23)[c]	0.00	846
CVFM	5	0.69 (0.53)	2.13	–
CVIM	1	2.08 (1.00)	0.00	985
CVIM	4	1.93 (0.84)	2.31	–
FTI-276	1	3.01 (1.75)	0.00	388
FTI-276	4	3.38 (1.95)	0.24	–
FTI-276	16	0.63 (0.44)	1.64	–
FTI-2148	1	3.29 (2.28)	0.00	501
FTI-2148	2	3.02 (1.82)	0.52	–
FTI-2148	6	1.37 (0.92)	3.85	-
L-739,750	1	1.04 (0.64)	0.00	284
R-115777	1	7.96 (3.45)	0.00	119
R-115777	2	5.45 (1.23)	6.48	–
DPI-1	1	1.53 (1.35)	0.00	26

The lowest energy structure (rank = 1) is listed and, if not the lowest energy structure, the structure with the best RMSD within 10 kJ/mol of the lowest energy structure is listed along with other specific structures discussed in this report.
[a]RMSDs were calculated for inhibitor non-hydrogen atoms by overlaying the X-ray structure of the inhibitor on the docked pose. Maestro was used for these "in place" RMSD calculations. For X-ray structures having different coordinate frames than the FTase/CVFM structure from which our binding site model was derived, Swiss PDB Viewer (version 3.7) was used to fit the FTase/inhibitor X-ray structure to the FTase/CVFM X-ray structure via superimposition of backbone atoms.
[b]Total number of poses obtained within a 25 kJ/mol energy window relative to the lowest energy structure.
[c]Numbers in parentheses represent least-squares superimposition RMSD's that were obtained when the docked inhibitor was rigidly superimposed (using Maestro) on the X-ray structure of the inhibitor that was employed as a template.

well as zinc and FPP are displayed. Hydrogen bonds between CVFM and FTase observed in our docked structure are also shown. A comparison of the LES with the X-ray structure is shown in Figure 2b (only slight adjustment of the flexible residues (not shown) and FPP (not shown) relative to the crystal structure had occurred). The 5th structure relative to the LES using 4r electrostatics shows remarkable agreement with the X-ray structure with an overlay RMSD relative to the crystal structure of 0.69 Å and a superimposition RMSD of 0.53 Å (Table 1). The comparison of this structure relative to the X-ray structure is shown in Figure 2c (only slight adjustment of the flexible residues (not shown) and FPP (not shown) relative to the crystal structure had occurred). It is worth noting that the energy of this structure is 2.13 kJ/mol higher than the LES, underscoring that approximations inherent in molecular mechanics based computational methodology may fail to identify the structure that most closely resembles the X-ray structure as the LES. Nevertheless, the energy of this structure is low relative to the X-ray structure. It is noteworthy that we were able to reproduce the crystal structure quite well using a non-bonded model for inhibitor ligation to zinc.

Examination of the docked poses for CVFM indicates that there is some limited conformational mobility of Try361β. Asp297β, Cys299β, His362β and zinc itself exhibit only very slight mobility as would be expected since Asp297β, Cys299β, and His362β are tethered to zinc. On the other hand, FPP is quite mobile.[5] Figure 3 shows an ensemble of structures obtained in our study and includes the LES and all structures within a 10 kJ/mol energy window relative to the LES and provides insight into the mobility of the flexible residues and FPP during the docking simulation with CVFM.

Our docking studies show numerous alternative conformations for the Met side chain suggesting that the methionine pocket can tolerate groups larger than methionine at the C-terminus of the peptide and suggesting alternative locations for the placement of side chains that may improve potency.

CVIM

Docking of CVIM and each of the other inhibitors shown in Figure 1 was then performed using the binding site model derived from the FTase/CVFM/FPP ternary complex and *4r electrostatics*

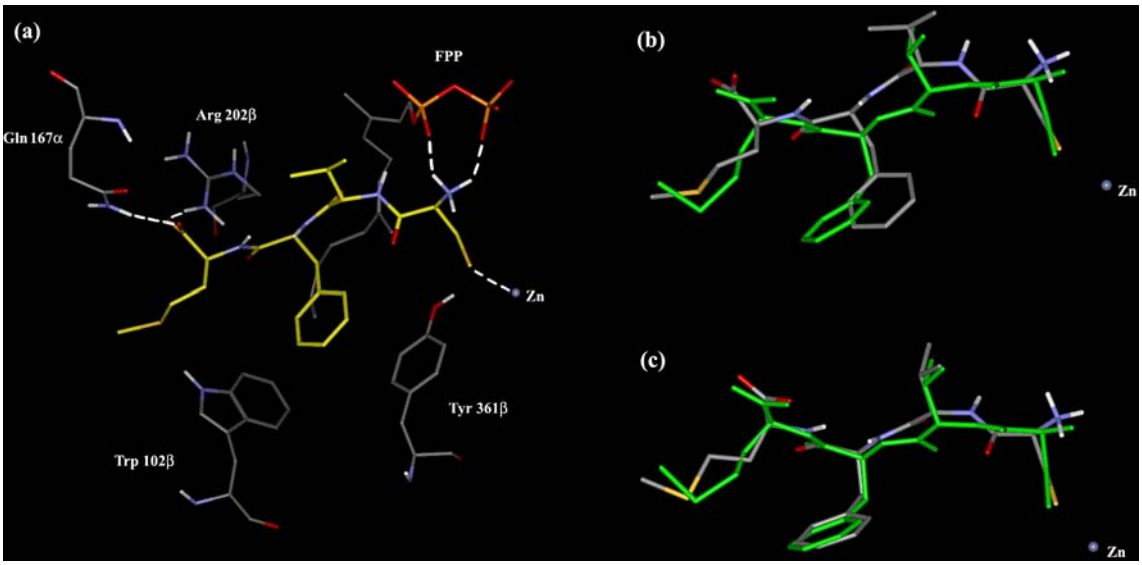

Figure 2. Panel a: CVFM (LES) docked to the catalytic site of FTase using 4r electrostatics. Carbon atoms of the inhibitor are shown in yellow and several key residues, FPP and the Zn(II) ion are shown as well. Hydrogen bonds between the C-terminal carboxyl group of CVFM and Arg202β and GLN167α and the N-terminal amino group and FPP are also shown. Panel b: CVFM (LES) vs. the X-ray structure (shown in green). Panel c: CVFM (5th lowest energy structure) vs. the X-ray structure (shown in green).

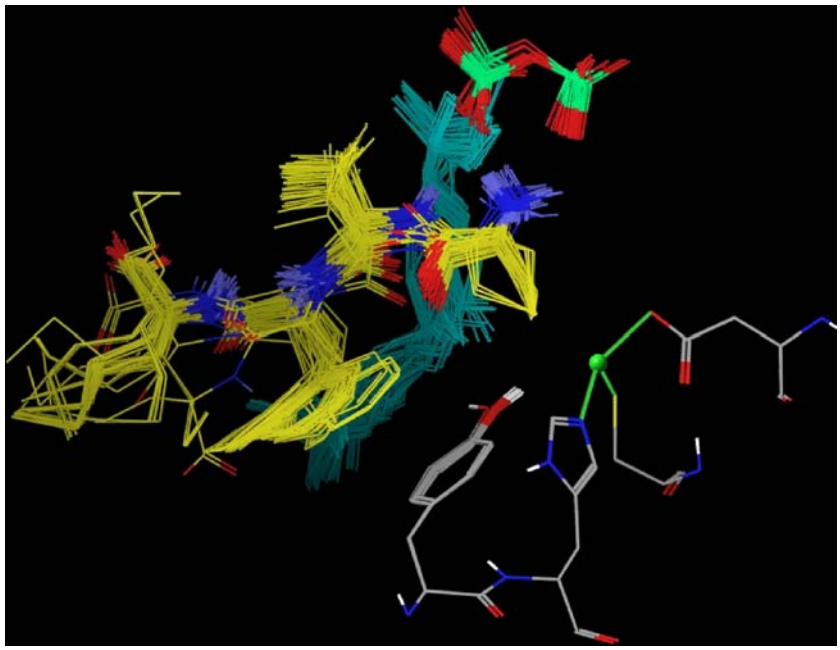

Figure 3. Overlay of the LES of CVFM and all structures within a 10 kJ energy window relative to the LES. Flexible residues, FPP and the Zn(II) ion are shown as well. Carbon atoms of CVFM are shown in yellow and carbon atoms of FPP are shown in turquoise.

was used in each case. Using Maestro, CVIM was manually positioned in the binding site model in a ''flipped'' orientation (like CVFM) after removal of the CVFM structure. Figure 4 shows our results for CVIM. Although the crystal structure of a CVIM analog (Acetyl-Cys-Val-Ile-Seleno-Met)

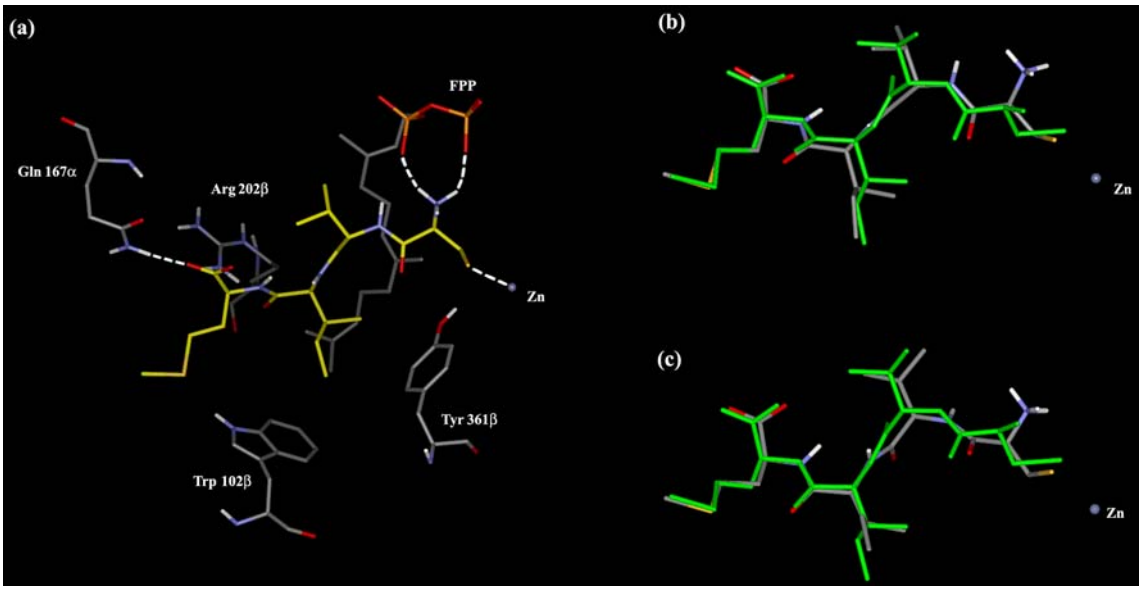

Figure 4. Panel a: CVIM (LES) docked to the catalytic site of FTase. Carbon atoms of the inhibitor are shown in yellow and several key residues, FPP and the Zn(II) ion are shown as well. Hydrogen bonds between the C-terminal carboxyl group of CVIM and GLN167α and the N-terminal amino group and FPP are also shown. Panel b: CVIM (LES) vs. the X-ray structure (shown in green). Note that the acetyl group in the X-ray structure has been removed for clarity. Panel c: CVIM (4th lowest energy structure) vs. the X-ray structure (shown in green). The acetyl group in the X-ray structure has been removed for clarity.

complexed to FTase has been determined [6] and is available from the Protein Databank [24], entry: 1QBQ, we chose to use our CVFM catalytic site model for the docking of CVIM to determine whether we could obtain docking modes that were in substantial agreement with the docking mode of Acetyl-Cys-Val-Ile-Seleno-Met determined crystallographically (often referred to as "cross docking"). In Figure 4a we show the LES and in Figure 4b, it is compared with the crystal structure of the CVIM analog. The overlay RMSD for the two structures is 2.08 Å and the superimposition RMSD is 1.00 Å (Table 1). Although there are some differences (most notably at the Val residue and the position of the N-terminal nitrogen atom), the docked structure is in good agreement with the crystal structure. The 4th lowest energy structure exhibited better agreement with the X-ray structure with an overlay RMSD of 1.93 Å and a superimposition RMSD of 0.84 Å (Table 1) and its comparison with the X-ray structure is shown in Figure 4c. Note that the superimposition RMSDs for the LES and 4th lowest energy structure are quite good, indicating that the *conformation* of each of these structures is in substantial agreement with the one observed crystallographically. It is noteworthy that the ternary complex used for the crystal structure not only contains an analog of CVIM but also an FPP analog (α-hydroxyfarnesylphosphonic acid). Thus, perfect agreement with the crystal structure would not have been expected. In particular, since we docked CVIM instead of the acetylated analog, our ensemble of docked structures typically show a hydrogen-bonded ion pair interaction between the N-terminal ammonium ion and FPP. Such an ion pair is not possible for Acetyl-Cys-Val-Ile-Seleno-Met. Moreover, the N-terminal acetamide N–H is not hydrogen-bonded to the FPP analog used for crystallography. Nonetheless, the agreement we observed provided sufficient justification for using the FTase/FPP/CVFM binding site model in subsequent studies. We point out that this would be a typical situation in a structure-based drug design project where the crystal structure of an initial complex would be used to design other inhibitors.

Peptidomimetics

FTI-276

We next turned our attention to one of our own inhibitors, FTI-276, for which we possess X-ray crystallographic information [15]. In FTI-276, the

two aliphatic amino acids in the CaaX motif are replaced with a 4-amino-2-phenylbenzamide spacer. Like the CaaX peptide inhibitors, FTI-276 is a thiol and we anticipated that like CVFM and CVIM, our methodology, in particular our zinc parameterization, would be able to provide reasonable docking modes. Maestro was used to generate a starting structure for FTI-276 (and the remainder of the inhibitors described in this study) by manually positioning each inhibitor in an arbitrary pose[1] within the binding site model derived from the FTase/CVFM/FPP ternary complex. The LES for FTI-276 compared modestly well with the X-ray structure with an overlay RMSD of 3.01 Å and a superimposition RMSD of 1.75 Å. However, in contrast to the X-ray structure, this structure failed to position any substituent within the hydrophobic pocket formed by residues Trp102β, Trp106β and Tyr361β and the terminal isoprene of FPP. It has been noted in the literature [13], that many potent inhibitors studied crystallographically possess hydrophobic (usually aromatic) substituents occupying this pocket. The phenylalanine residue in CVFM provides an example. Interestingly the 4th lowest energy structure did place the *ortho*-phenyl substituent attached to the *para*-amino benzamide moiety of FTI-276 in this hydrophobic pocket. In Figure 5a, we show this structure docked into the FTase catalytic site. The structure has an overlay RMSD of 3.38 Å and superimposition RMSD of 1.95 Å relative to the X-ray structure (Table 1). In Figure 5b, we show a comparison of this structure and the X-ray structure. The docked structure shown in Figure 5a differs from the X-ray structure mostly in placement of the methionine side chain. In our docked structure, both the Met side chain and the *para*-phenyl group of the 4-amino-2-phenylbenzamide spacer reside in the hydrophobic pocket mentioned above and the *para*-phenyl group has positioned itself within the pocket to accommodate the methionine. We already noted that our docking studies show numerous alternative conformations for the Met side chain and in our docked structure it has ''moved'' into the previously described hydrophobic pocket. Remarkably, one of the structures of lowest energy using 4r electrostatics (ΔE = 1.64 kJ/mol, and ranked 16th relative to the LES) is almost identical to the X-ray structure (Figure 5c), with an overlay RMSD of 0.64 Å and a superimposition RMSD of 0.44 Å (Table 1).

FTI-2148

We also decided to dock another inhibitor of ours, FTI-2148, for which we also possess X-ray

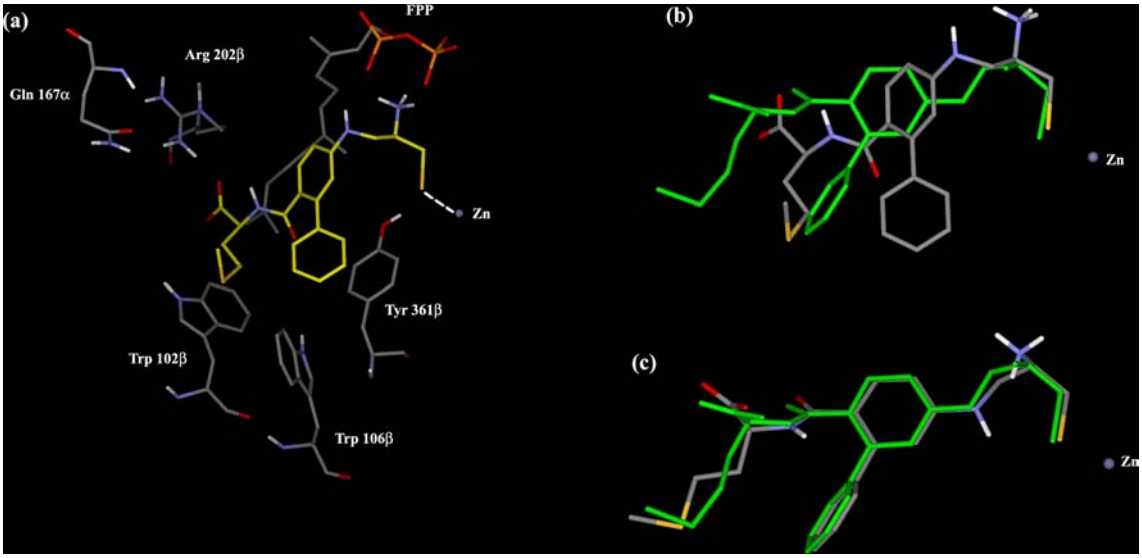

Figure 5. Panel a: FTI-276 (4th lowest energy structure) docked to the catalytic site of FTase. Carbon atoms of the inhibitor are shown in yellow and several key residues, FPP and the Zn(II) ion are shown as well. Panel b: FTI-276 (4th lowest energy structure) vs. the X-ray structure (shown in green). Panel c: FTI-276 (16th lowest energy structure) vs. the X-ray structure (shown in green).

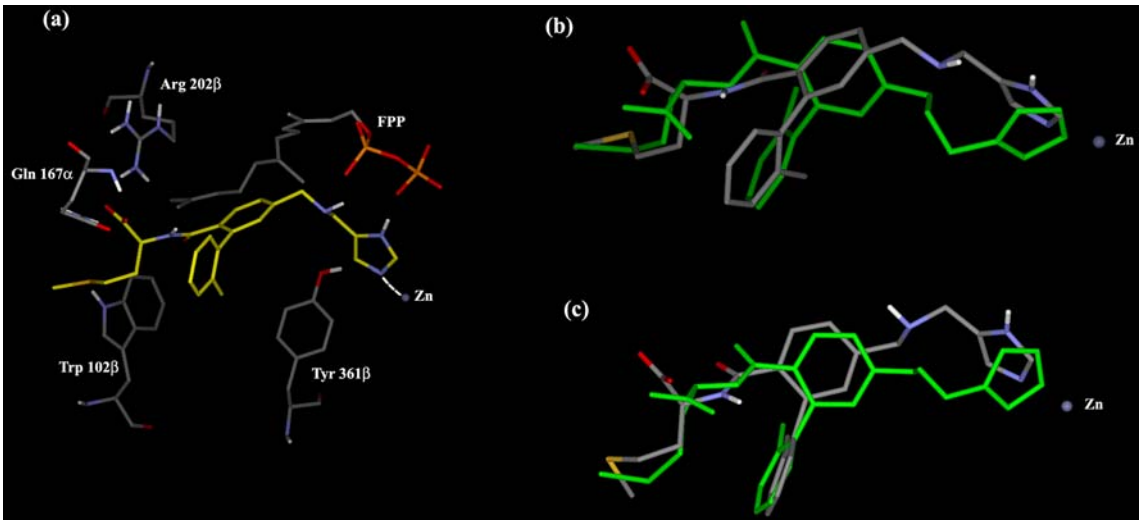

Figure 6. Panel a: FTI-2148 (2nd lowest energy structure) docked to the catalytic site of FTase. Carbon atoms of the inhibitor are shown in yellow and several key residues, FPP and the Zn(II) ion are shown as well. Panel b: FTI-2148 (2nd lowest energy structure) vs. X-ray structure (shown in green). Panel c: FTI-2148 (6th lowest energy structure) vs. the X-ray structure (shown in green). Note that the methyl group in the tolyl ring is pointed toward the "back" in both the X-ray structure and in structure 6.

crystallographic information [15]. Figure 6a shows the 2nd lowest energy structure we observed and Figure 6b shows the comparison to the X-ray structure. This structure shows reasonable agreement with the X-ray structure (overlay RMSD = 3.02 Å; superimposition RMSD = 1.82 Å; Table 1). The 2nd lowest energy structure is only a few tenths of a kJ/mol higher in energy (ΔE = 0.52 kJ) than the LES and is identical to it with the exception that the phenyl group of the tolyl ring is rotated so that the methyl group is pointing (instead of the "front") toward the "back" as is the case with the X-ray structure (Figure 6b). Our modeling studies would be consistent with both rotamers being populated. Figure 6c shows a comparison of the X-ray structure with the 6th lowest energy structure using 4r electrostatics (ΔE = 3.85 kJ relative to the LES). This structure shows excellent agreement with the X-ray structure (overlay RMSD = 1.37 Å; superimposition RMSD = 0.92 Å; Table 1).

It is particularly noteworthy that our modeling studies show that ligation of FTI-2148 to zinc is through its imidazole moiety (as the crystal structure also demonstrates) since our parameters for zinc were optimized for thiols. Our simulations with FTI-2148 reveal that in the structure most closely resembling the X-ray structure (structure 6) the sum of the van der Waals and electrostatic energies for the imidazole N–Zn interaction is −45.97 kJ/mol whereas in structure 5 of CVFM (again, the structure closest to the X-ray structure), it is −68.37 kJ/mol for the S–Zn interaction. Thus, although weaker than the thiolate zinc interaction, ligation to zinc in FTI-2148 was, nonetheless, observed to occur with imidazole (as opposed to the carboxylate, for example).

An "extra radius" surface rendering of the protein (Figure 7) shows the hydrophobic surface available to the phenyl group of CVFM and the tolyl ring of FTI-2148. The extensive volume bounded by this surface indicates that larger groups than phenyl or tolyl may readily be accommodated by this pocket. It has already been noted that our docking algorithm with FTI-276 attempts to place both the phenyl group and the methionine side chain of FTI-276 into this large, mostly hydrophobic pocket. That this pocket can tolerate larger groups than phenyl is consistent with experimental data. An analog of FTI-276 with a naphthyl substituent replacing this phenyl group is quite active (IC_{50} = ~2 nM; unpublished data), but about four fold less potent than FTI-276.

L739,750

Our docking studies with L739, 750 afforded an ensemble of low energy structures that suggest that this compound docks in fashion that is very similar to CVFM. The same pockets in the enzyme are

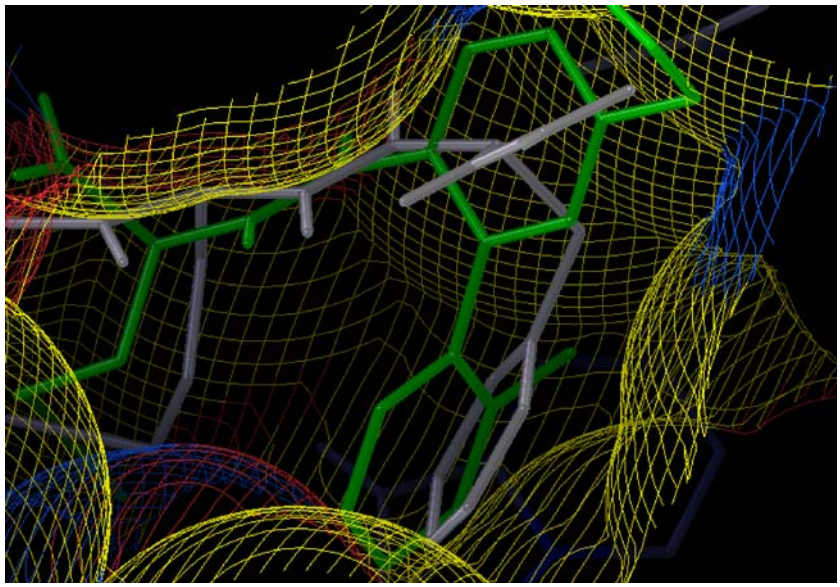

Figure 7. Extra radius surface of the FTase catalytic site which also shows FTI-2148 (structure 6, shown in green) and the CVFM X-ray structure (shown in grey). Yellow portions of the mesh represent regions of the surface adjacent to non-polar atoms in the catalytic site. Blue surface patches show where atoms that are H-bond acceptors are located in the catalytic site; red surface patches indicate the presence of H-bond donors in the catalytic site. An "extra radius" surface, also known as a Lee and Richards surface is useful in drug design since it nicely depicts the volume available to a skeletal model (i.e., stick figure) of the ligand.

occupied by similar groups in the low energy docked poses. For example, the benzyl group occupies the hydrophobic pocket into which the phenylalanine side chain from CVFM fits. Moreover, like CVFM, the low energy structures bind in an extended conformation with the cysteine thiolate ligated to zinc. A comparison of the LES to the X-ray structure [10] of L739-750 (taken from the Protein Databank [24], entry: 1JCQ) shows excellent agreement between the two structures (overlay RMSD = 1.04 Å; superimposition RMSD = 0.64 Å; Table 1). In Figure 8a we show the LES and in Figure 8b we show its comparison with the X-ray structure.

Non-peptidomimetics

R-115777

We decided to examine the FTase inhibitor R-115777 (Zarnestra), developed by J & J Pharmaceuticals, which is currently in clinical trials [26] as an anticancer agent, and has been studied crystallographically as a ternary complex with FTase and FPP [13]. As expected, based on our modeling of FTI-2148, the methyl–imidazole group was found to be ligated to zinc in the low energy docking modes. Unfortunately, other than this zinc ligation by the methyl–imidazole substituent, the LES did not compare very favorably with the X-ray structure (taken from the Protein Databank [24], entry: 1SA4; overlay RMSD = 7.96 Å; superimposition RMSD = 3.45 Å; Table 1). Of the structures with relatively low energy (i.e., within a 10 kJ energy window of the LES), the 2nd lowest energy structure possessed the best fit to the X-ray structure with an overlay RMSD of 5.45 Å and a superimposition RMSD of 1.23 Å. In fact, although there were structures similar to the 2nd lowest energy structure in the total ensemble of structures within 25 kJ/mol, none matched the X-ray structure with better fidelity. As can be ascertained from the favorable superimposition RMSD, the conformation of this structure compares quite well with the X-ray structure. The overall pose, however, differs from the X-ray structure primarily due to the fact that the amino substituent in the docked pose (modeled as the 1° ammonium ion) forms two hydrogen bonds to the pyrophosphate moiety of FPP. In the X-ray structure, such direct hydrogen bonding is not seen, and a water mediated hydrogen bond to the α-phosphate of FPP is observed instead. Thus, in R-115777, the docked

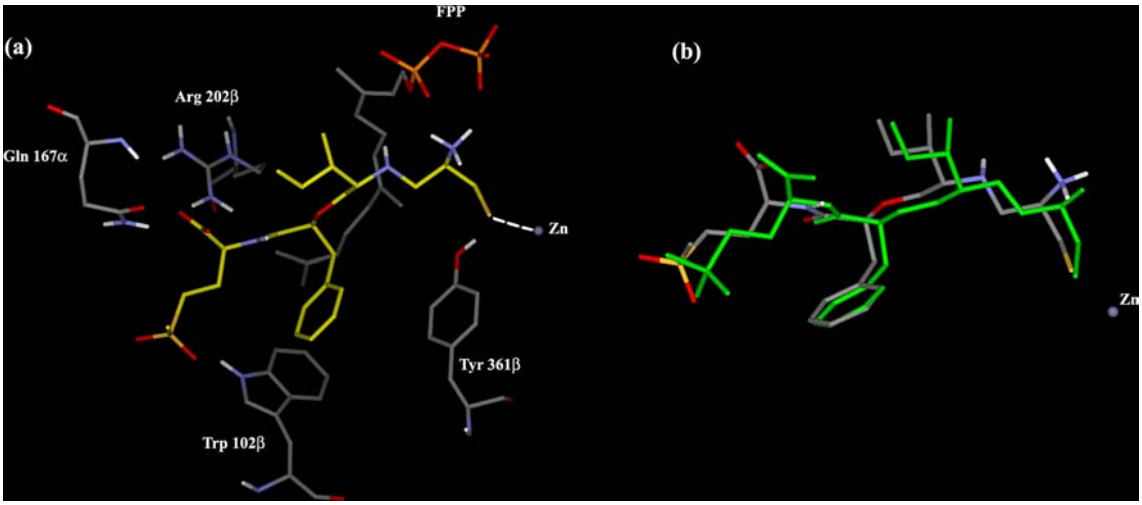

Figure 8. L739,750 (LES) docked to the catalytic site of FTase. Carbon atoms are shown in yellow and several key residues, FPP and the Zn(II) ion are shown as well. Panel b: L739,750 (LES) vs. the X-ray structure (shown in green).

pose is substantially tilted relative to the X-ray structure. In Figure 9a we show this 2nd lowest energy docked structure and in Figure 9b it is compared to the X-ray structure. Interestingly, in the crystallographically observed structure, the methyl group of the methyl–imidazole substituent is directed toward the isoprene substructure of FPP, whereas it is directed away from FPP in the structure shown in Figures 8a, b.

It is noteworthy that it is observed crystallographically that much of the R-115777 molecule interacts with hydrophobic residues (e.g., Trp102β, Trp106β and Tyr361β) and the hydrocarbon portion of FPP. In our 2nd lowest energy structure,

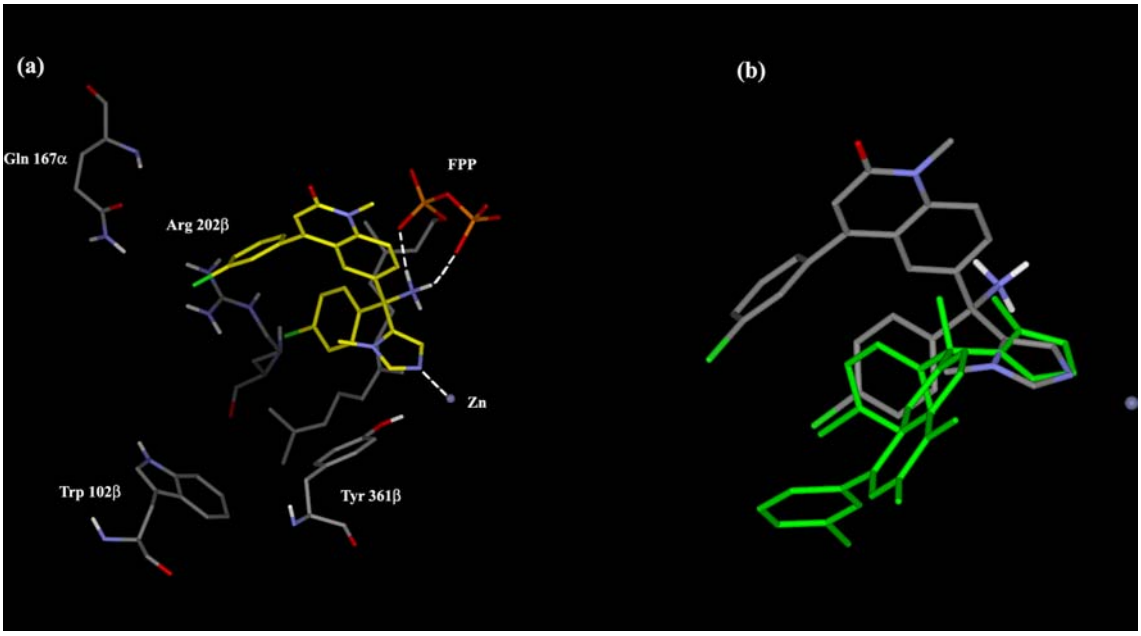

Figure 9. Panel a: R-115777 (2nd lowest energy structure) docked to the catalytic site of FTase. Carbon atoms of the inhibitor are shown in yellow and several key residues, FPP and the Zn(II) ion are shown as well. Hydrogen bonds between the amino group and FPP are shown. Panel b: R-115777 (2nd lowest energy structure) vs. the X-ray structure (shown in green).

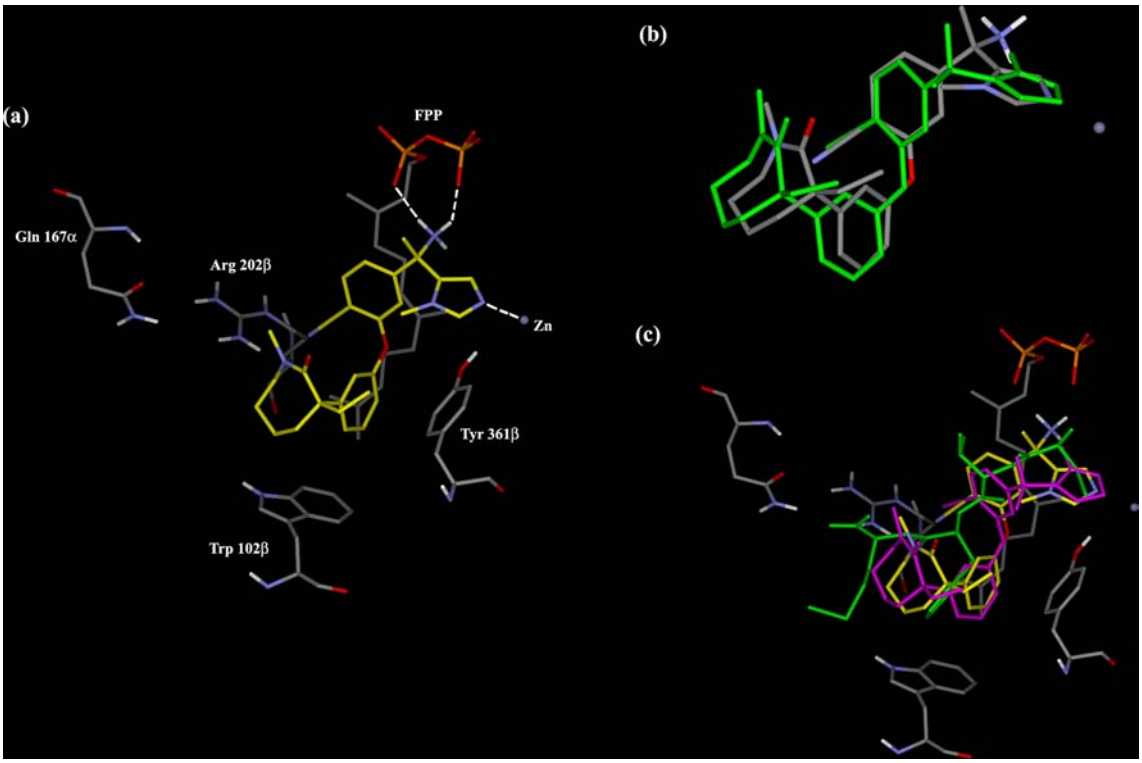

Figure 10. Panel a: DPI-1 (LES) docked to the catalytic site of FTase. Carbon atoms of the inhibitor are shown in yellow and several key residues, FPP and the Zn(II) ion are shown as well. Hydrogen bonds between the amino group and FPP are shown. Panel b: DPI-1 (lowest energy structure) vs. the X-ray structure (shown in green). Panel c: DPI-1 (LES) docked to the catalytic site of FTase. Carbon atoms of DPI-1 are shown in yellow and several key residues, FPP and the Zn(II) ion are shown as well. The X-ray structures of CVFM (shown in green) and DPI-1 (shown in purple) are also shown.

only the *para*-chloro substituent interacts with Tyr361β and the hydrophobic portion of FPP. It appears that it is difficult for R-115777, which is relatively rigid, to adopt an orientation in which optimal hydrophobic interactions can take place if two direct hydrogen bonds occur between the amino group of the molecule and the pyrophosphate moiety of FPP.

It is somewhat surprising that this compound does not possess any substituents that occupy the Met binding pocket. The potency of this compound is most likely due to its rigidity and relative orientation of the chlorophenyl substituents, which allows them to be pre-organized for optimal interaction with the farnesyl group of FPP and hydrophobic aromatic residues.

DPI-1

The dual FTase/geranylgeranyl transferase inhibitor, DPI-1, described by scientists at Merck Pharmaceuticals [27] was of interest to us. Our docking simulations yielded an ensemble of structures in which the LES was in excellent agreement with the X-ray structure [14] (taken from the Protein Databank [24], entry: 1MZC) with an overlay RMSD of 1.53 Å and a superimposition RMSD of 1.35 Å (Table 1). This structure is shown in Figure 10a. As expected, based on our modeling of FTI-2148, the imidazole group is ligated to zinc and comparison of the LES with the X-ray structure is shown in Figure 10b. Like R-115777, the amino group of DPI-1 (modeled as the 1° ammonium ion) forms two hydrogen bonds with FPP in the LES. Astonishingly, in the X-ray structure there are no such hydrogen bonds, not even water mediated hydrogen bonds. Also, like R-115777, the methyl group of the methyl–imidazole substituent is directed toward the isoprene substructure of FPP in the X-ray structure, whereas it is directed away from FPP in the LES. Unlike R-115777, the LES for DPI-1 is able to adopt an orientation and conformation that very much

resembles the X-ray structure (Figure 10b) in spite of being tethered to FPP via two hydrogen bonds that are not observed crystallographically.

Interestingly, in spite of its excellent potency (IC_{50} = 0.05 nM), the ε-lactam moiety only partially occupies the methionine binding pocket as is depicted in Figure 10c where we show the LES and X-ray structure for DPI-1 compared with the X-ray structure of CVFM. As with the methionine in CVFM, we observed several alternative binding conformations for the ε-lactam substituent. Our conclusion, initially based on our docking studies with CVFM, that the methionine pocket can tolerate groups larger than a Met side chain seems (at least in part) to be observed with this substituent.

Conclusion

We have used a single binding site model derived from the crystal structure of CVFM to dock CVFM, CVIM and the range of structures shown in Figure 1. We have been able to ascertain from docking studies with CVFM that 4r electrostatics significantly outperforms 2r electrostatics in locating low energy structures resembling the X-ray structure. Moreover, from our studies it appears that 10,000 step Low Mode searches[4] are sufficient, in general, at locating low energy structures that are in agreement with the ones observed by X-ray crystallography. Although a relatively large number of poses are obtained for highly flexible inhibitors (see Table 1), in most cases we obtained excellent agreement between the X-ray structure and either the LES or one of the lowest energy structures.

Our study included a diverse set of inhibitors (including non-thiols) and represents a challenging problem for several reasons. First, although we allow some limited protein flexibility in our docking simulations, larger scale protein conformational mobility (relative to the FTase/CVFM/FPP complex) that may accompany binding of some inhibitors could potentially be inadequately accounted for. Secondly, crystallographic water molecules were removed from the FTase/CVFM/FPP complex, which was then used to build the truncated model used for all of the docking simulations performed in this study. Although for most of the inhibitors studied, removal of crystallographic waters yielded a binding site model that afforded reasonable docked poses, for R-115777 this omission proved to be problematic. Finally, zinc parameterization of the AMBER* force field was done using a truncated FTase/CVFM model with a thiol inhibitor (i.e., CVFM) and a non-bonded model was employed for inhibitor ligation to zinc. Given these, and other, approximations to the docking methodology we employed, it is not surprising that the LES is not the structure in each and every case that agrees most closely with the X-ray structure. Nor is it surprising that we were unable to model R-115777 very well since our methodology is unable take water mediated hydrogen bonds (like the one observed crystallographically for this inhibitor) into account. The fact that we have been able to reproduce the X-ray structures of inhibitors that ligate to zinc via imidazoles is particularly noteworthy since our parameters for zinc were optimized for thiolates like CVFM.

An important finding from our docking studies is that a number of alternative conformations for the methionine side chain in the peptide inhibitors can be accommodated by the enzyme binding site. Examination of the docking modes for methionine containing inhibitors shows alternative energetically allowed locations for the Met side chain and may suggest substituents that can be incorporated into lead inhibitors to improve potency. Moreover, a number of alternative conformations were observed for the ε-lactam moiety in DPI-1, which was found to at least partially occupy the methionine binding pocket. These results suggest that the methionine binding pocket can tolerate fairly large groups (e.g., groups larger than methionine). Interestingly, R-115777 does not posses a substituent that occupies the methionine binding pocket at all, suggesting that the potency of this compound could be improved by the addition of such a substituent.

In summary, using a single binding site model we have been able to perform docking simulations that generally afford low energy structures that are in agreement with the ones observed crystallographically. Although approximate, we believe that we have validated the use of the docking methodology described in this report for the design of improved FTase inhibitors. Furthermore, using this methodology we believe that ongoing studies in our laboratories will result in the design of even more potent and more selective FTase inhibitors than are currently available.

Notes

1. It should be noted that, in general, one would most likely have a reasonable hypothesis about the docked geometry of a particular inhibitor and would use this geometry as a starting pose. For zinc metalloenzymes, in particular, the number of zinc binding groups will be quite limited and the atoms that will be ligated to zinc in the complex may very well be known in advance. Thus, arbitrary positioning of the starting pose is too stringent a criterion for selecting a starting geometry in most cases.
2. The elimination of duplicates by MacroModel takes molecular symmetry into account and considers two structures to be the equivalent if after rigid body least-squares superimposition of atoms selected by the user for comparison, no atomic displacement between corresponding atoms is greater than an adjustable value of 0.25 Å.
3. An examination of one of these docking simulations after 1500 steps indicated that a very diverse number of docking poses were being explored including ones that had the C-terminal methionine carboxylate and the phenylalanine carbonyl (in addition to the cysteine thiolate) coordinated to zinc.
4. We cannot claim in the docking studies we report that exhaustive (i.e., converged) searches have been performed. In fact, much longer searches (in excess of 50,000 steps, starting with the ''flipped'' CVFM structure) have recently been performed using MacroModel 8.6. As anticipated, additional conformations were discovered. Nonetheless, in those searches using 4r electrostatics, the final ensemble still contains low energy structures closely related to the X-ray structure whereas there are no such structures with 2r electrostatics.
5. Initial docking simulations with FPP fixed at its crystallographically observed position in CVFM were not as effective at locating low energy structures that matched the X-ray structures of CVFM or several other inhibitors used in this study.

Acknowledgments

We thank the National Institutes of Health (CA67771) for financial support of this work. We also thank Dr. Corey Strickland of Schering Plough for supplying us with the coordinates of the X-ray structures of FTI-276 and FTI-2148. We thank Mr. Matt Maderios of Eckerd College for assistance with the docking studies performed on DPI-1.

References

1. Gibbs, J.B., Oliff, A. and Kohl, N.E., Cell, 77 (1994) 175.
2. Zhu, K., Hamilton, A.D. and Sebti, S.M., Curr. Opin. Investig. Drugs, 4 (2003) 1428.
3. Sebti, S.M. and Der , C.J., Nature Rev. Cancer, 3 (2003) 945.
4. Bell, I.M., Exp. Opin. Ther. Patents, 10 (2000) 1813.
5. Park, H.W., Boduluri, S.R., Moomaw, J.F., Casey, P.J. and Beese, L.S., Science, 275 (1997) 1800.
6. Strickland, C.L., Windsor, W.T., Syto, R., Wang, L., Bond, R., Wu, Z., Schwartz, J., Le, H.V., Beese, L.S. and Weber, P.C., Biochemistry, 37 (1998) 16,601.
7. Long, S.B., Casey, P.J. and Beese, L.S., Biochemistry, 37 (1998) 9612.
8. Dunten, P., Kammlott, U., Crowther, R., Weber, D., Palermo, R. and Birktoft, J., Biochemistry, 37 (1998) 7907.
9. Long, S.B., Casey, P.J. and Beese, L.S., Struct. Fold Des., 8 (2000) 209.
10. Long, S.B., Hancock, P.J., Kral, A.M., Hellinga, H.W. and Beese, L.S., Proc. Natl. Acad. Sci. U.S.A., 98 (2001) 12,948.
11. Long, S.B., Casey, P.J. and Beese, L.S., Nature, 419 (2002) 645.
12. Turek-Etienne, T.C., Strickland, C.L. and Distefano, M.D., Biochemistry, 42 (2003) 3716.
13. Reid, T.S and Beese, L.S., Biochemistry, 43 (2004) 6877.
14. deSolms, S.J., Ciccarone, T.M., MacTough, S.C., Shaw, A.W., Buser, C.A., Ellis-Hutchings, M., Fernandes, C., Hamilton, K.A., Huber, H.E., Kohl, N.E., Lobell, R.B., Robinson, R.G., Tsou, N.N., Walsh, E.S., Graham, S.L., Beese, L.S. and Taylor, J.S., J. Med. Chem., 46 (2003) 2973.
15. Ohkanda, J., Strickland, C.L., Blaskovich, M.A., Carrico, D., Lockman, J.W., Vogt, A., Bucher, C.J., Sun, J., Qian, Y., Knowles, D., Pusateri, E.E., Sebti, S.M. and Hamilton, A.D., Organic Biomol. Chem. (In press).
16. Mohamadi, F., Richards, N.G.J., Guida, W.C., Liskamp, R., Lipton, M., Caufield, C., Chang, G., Hendrickson, T. and Still, W.C., J. Comput. Chem. 11 (1990) 11, 440; MacroModel, Schrödinger L.L.C. (www.schrodinger.com), New York, NY, USA.
17. Kolossvary, I. and Guida, W.C., J. Comp. Chem., 20 (1999) 1671.
18. FLO, Thistlesoft, Colebrook, CT, USA.
19. Bohacek, R.S. and McMartin, C., J. Med. Chem., 35 (1992) 1671.
20. Viewer Lite, Accelrys, Inc. (www.accelrys.com), San Diego, CA, USA.
21. Guida, W.C., Bohacek, R.S. and Erion, M.D., J. Comp. Chem., 13 (1992) 214.
22. Hoops, S.C., Anderson, K.W. and Merz, K.M., J. Am. Chem. Soc., 113 (1991) 8262.
23. Jaguar, Schrödinger L.L.C. (www.schrodinger.com), New York, NY, USA.

24. Berman, H.M., Westbrook, J., Feng, Z., Gilliland, G., Bhat, T.N., Weissig, H., Shindyalov, I.N. and Bourne, P.E., Nucleic Acids Res., 28 (2000) 235.
25. Saunders, M., Houk, K.N., Wu, Y.-D., Still, W.C., Lipton, M., Chang, G. and Guida, W.C., J. Am. Chem. Soc., 112 (1990) 1419.
26. Lancet, J.E., Rosenblatt, J.D., Liesveld, J.L. et al., Proc. Am. Soc. Clin. Oncol. (2000) 19.
27. Lobell, R.B., Omer, C.A., Abrahams, M.T. et al., Cancer Res., 61 (2001) 8758.